Supporting Information

Modulating electronic structure of ternary transition metal phosphide for enhanced hydrogen evolution activity

Sheying Dong[a*], Huangcong Tang[a], Kangkang Wang [a], Qian Zheng[a], Tinglin Huang [b]

[a] *School of Chemistry and Chemical Engineering, Xi'an University of Architecture and Technology, Xi'an 710055, People's Republic of China*

[b] *School of Environmental and Municipal Engineering, Xi'an University of Architecture and Technology, Xi'an 710055, People's Republic of China*

Corresponding author E-mail address: dongsyy@126.com

Electrochemical tests:

All electrochemical measurements were investigated in a standard three-electrode configuration on the electrochemical workstation (CHI660B, Shanghai Chenhua Instrument Co., Ltd., China) with 0.5 M H_2SO_4 used as the electrolyte in room temperature. The catalyst ink consists of a mixture of 5 mg catalyst powder, 800 μL deionized water, 150 μL ethanol, and 50 μL 0.5 wt% Nafion solution. Then the catalyst ink was under sonication for forty minutes. The black mixture ink was dropped onto the glassy carbon electrode in a mass loading of 0.354 mg/cm^2, dry for several hours to ensure the catalyst powder did not fall easily before measurement. A double salt bridge calomel electrode and graphite rod were utilized as the reference and counter electrode, respectively. The hydrogen evolution reactions (HER) performance was measured by polarization curve, obtained from linear sweep voltammetry (LSV) at a scan rate of 5 mV/s with 95% *iR*-correction.

For all electrochemical measurements, the electrochemical potential values for the three-electrode system were analyzed with the following equation from *E* (SCE) to *E* (RHE)

$$E\,(vs.\,\mathrm{RHE}) = E\,(vs.\,\mathrm{SCE}) + 0.2415 + 0.059 \times \mathrm{pH}$$

Electrochemical impedance spectroscopy (EIS) was recorded at the overpotential of 100 mV in a frequency range from 0.01 Hz to 100 kHz. The durability test of FeCoNiP@NCNTs was conducted with a chronoamperometric curve at a certain current density. Tafel plots are fitted to the Tafel equation:

$$\eta = \mathrm{b}\log j + a$$

where η is the overpotential, b is the Tafel slope, j is the current density and a is the Tafel intercept relative to the exchange current density j_0. The electrochemically active surface area (ECSA) was measured by Cyclic voltammetry (CV)-based electrochemical double layer capacitance (C_{dl}) measurements at the range of 10-100 mV s^{-1}. The ECSA was calculated by the following equation:

$$ECSA = \frac{C_{dl}}{40\mu F \mathrm{cm}^{-2}} cm^2_{ECSA}$$

Computational method

The equilibrium lattice constants of orthorhombic FeP unit cell were optimized, when using a 7×9×5 Monkhorst–Pack k-point grid for Brillouin zone sampling, to be a=5.109 Å, b= 3.011 Å, a=5.725 Å. We then use it to construct a FeP (002) surface model (model 1) with p(1×3) periodicity in the x and y directions and 3 stoichiometric layers in the z direction separated by a vacuum layer in the depth of 15 Å in order to separate the surface slab from its periodic duplicates. This surface model contains 36 Fe and 36 P atoms. In the the other model, Co and Ni atoms were doped into model 1 by replacing one Fe atom on the outmost layer, respectively. During structural optimizations, the gamma point in the Brillouin zone was used for k-point sampling, and the bottom two stoichiometric layers were fixed while the top one was allowed to relax. We build a FeP (002) surface model (model 2) with p (2×2) periodicity in the x and y directions and 3 stoichiometric layers in the z direction separated by a vacuum layer in the depth of 15 Å in order to separate the surface slab from its periodic duplicates. model 2 contains 48 Fe and 48 P atoms. During structural optimizations, the gamma point in the Brillouin zone was used for k-point sampling, and the bottom

two stoichiometric layers were fixed while the top one was allowed to relax.

The free energy of a gas phase molecule or an adsorbate on the surface was calculated by the equation G = E + ZPE − TS, where E is the total energy, ZPE is the zero-point energy, T is the temperature in kelvin (298.15 K is set here), and S is the entropy.

The free energy of adsorption (G_{ads}) of H atom was defined as

$$G_{ads} = G_{H/surf} - G_{H_2(g)/2}$$

where $G_{H/surf}$, G_{surf} and $G_{H_2(g)/2}$ are the free energy of H adsorbed on the surface, the free energy of clean surface, and the free energy of isolated H_2 molecule in a cubic periodic box with a side length of 20 Å and a 1×1×1 Monkhorst-Pack k-point grid for Brillouin zone sampling, respectively.

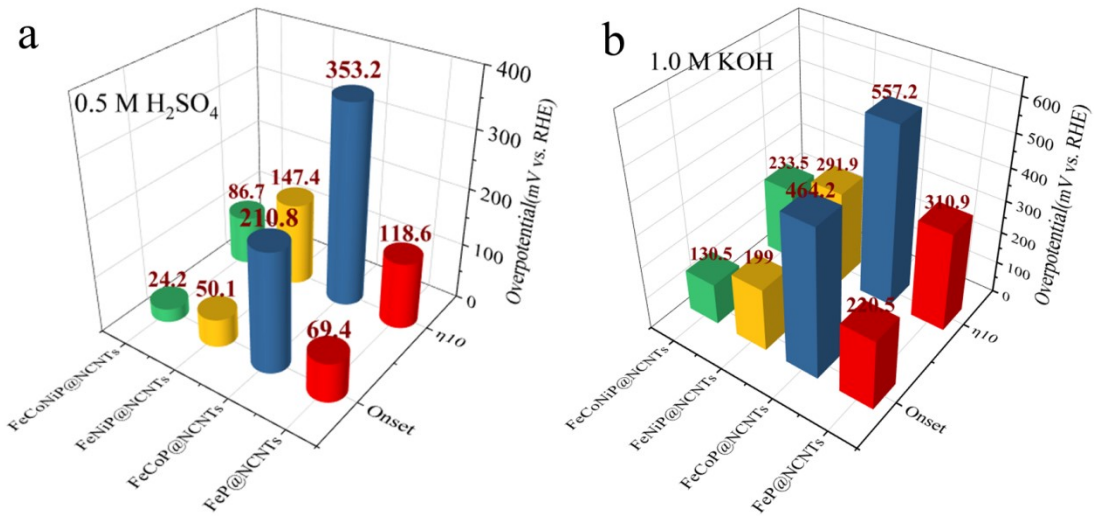

Fig. S1 The required overpotential at onset, and η_{10} of FeCoNiP@NCNTs in 0.5 M H_2SO_4 (a) and 1 M KOH (b).

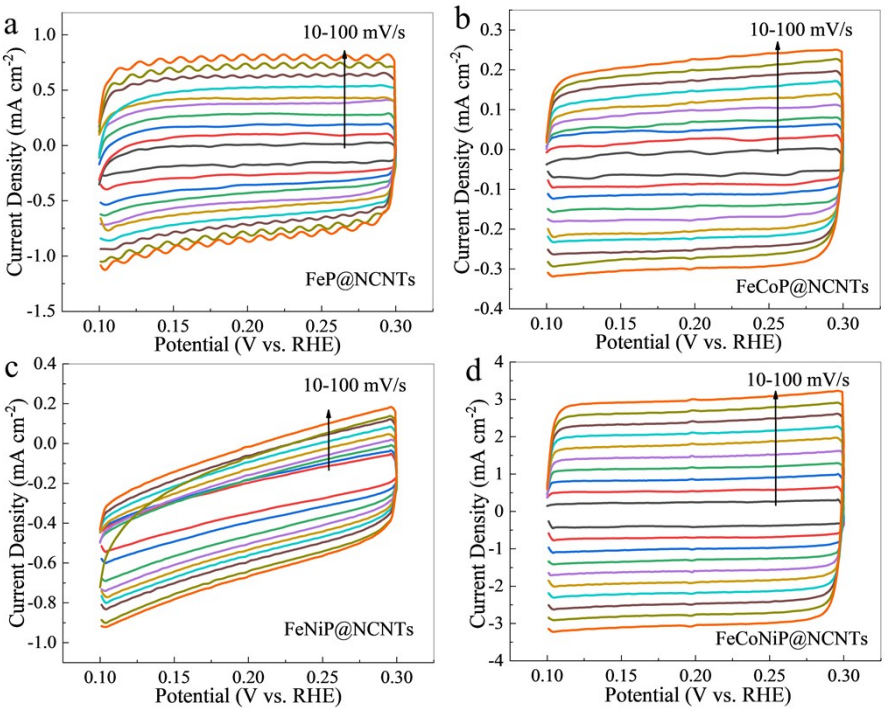

Fig. S2 The CV curves at different scan rates of (a) FeP@NCNTs, (b) FeCoP@NCNTs, (c) FeNiP@NCNTs, and (d) FeCoNiP@NCNTs in 0.5 M H_2SO_4.

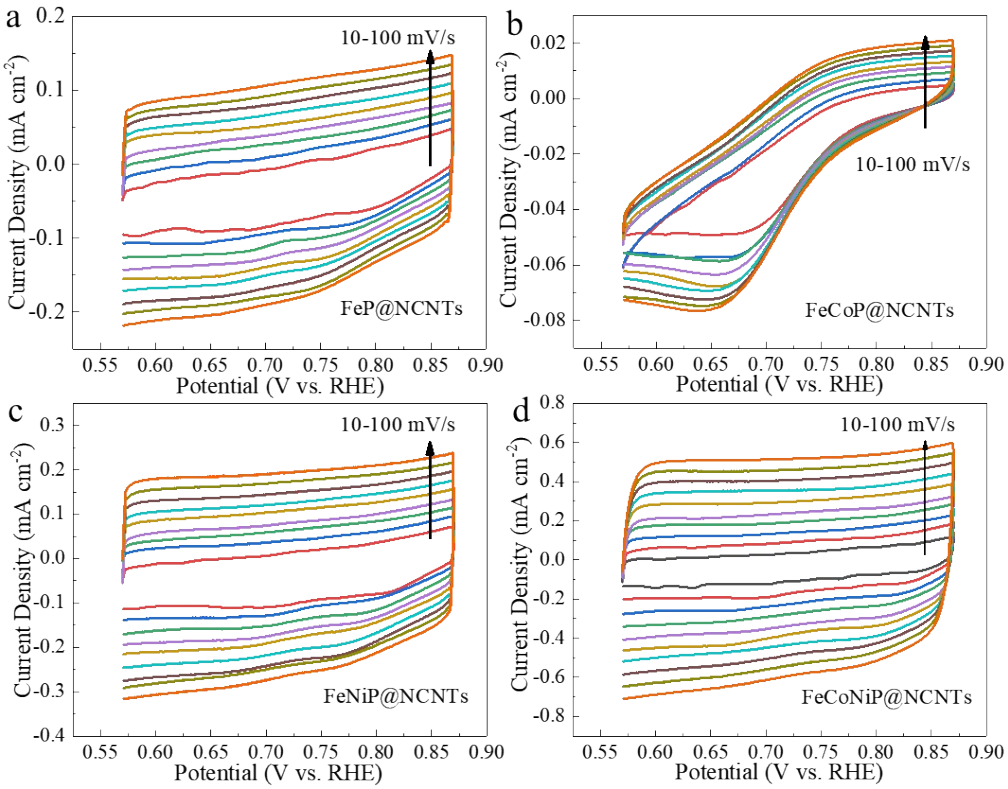

Fig. S3 The CV curves at different scan rates of (a) FeP@NCNTs, (b) FeCoP@NCNTs, (c) FeNiP@NCNTs, and (d) FeCoNiP@NCNTs in 1.0 M KOH.

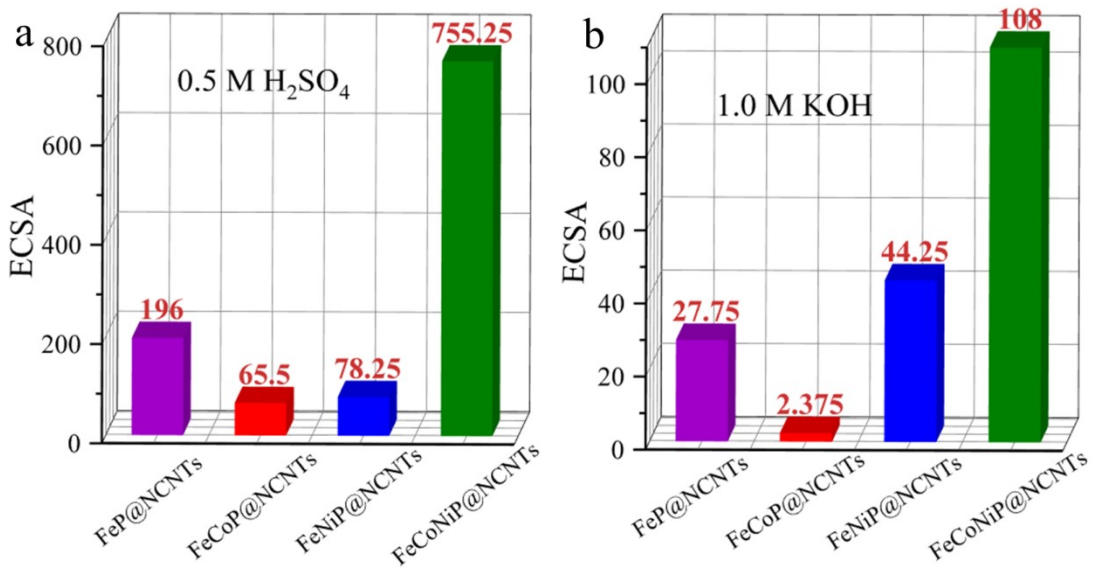

Fig. S4 ECSA of FeP@NCNTs, FeCoP@NCNTs, FeNiP@NCNTs, and FeCoNiP@NCNTs in 0.5 M H_2SO_4 (a) and 1.0 M KOH (b).

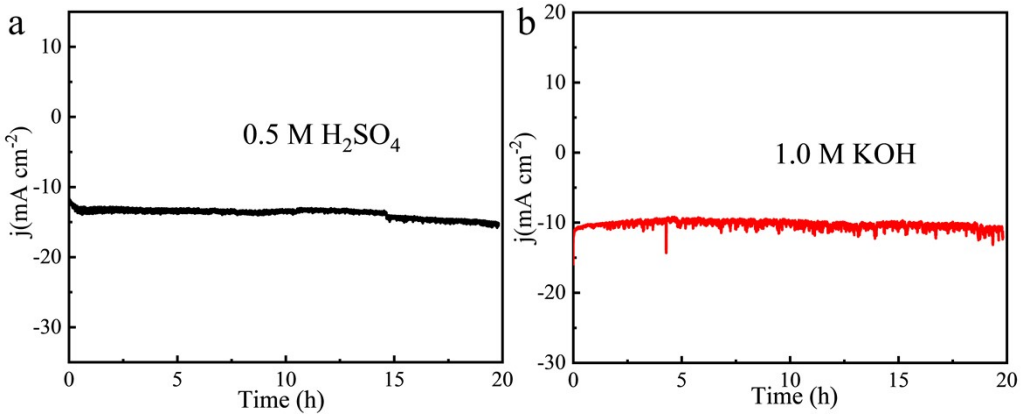

Fig. S5 Chronoamperometry of FeCoNiP@NCNTs in 0.5 M H_2SO_4 (a) and 1.0 M KOH (b).

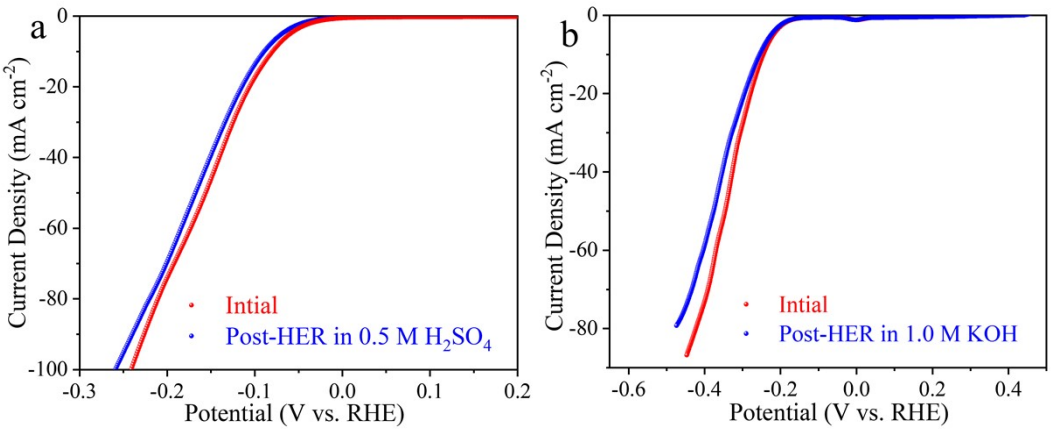

Fig. S6 LSV curves before and after stability tests in 0.5 M H_2SO_4 and 1.0 M KOH.

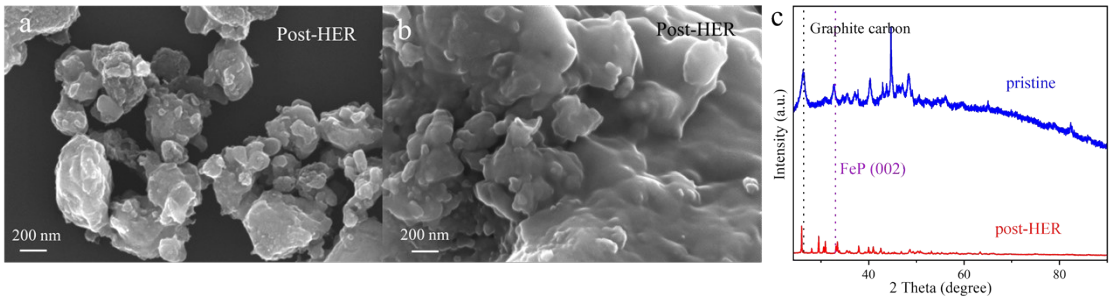

Fig. S7 The SEM images (a, b) and XRD pattern (c) of the post-HER FeCoNiP@NCNTs catalyst after the stability test for 20 h at 10 mA cm^{-2}.

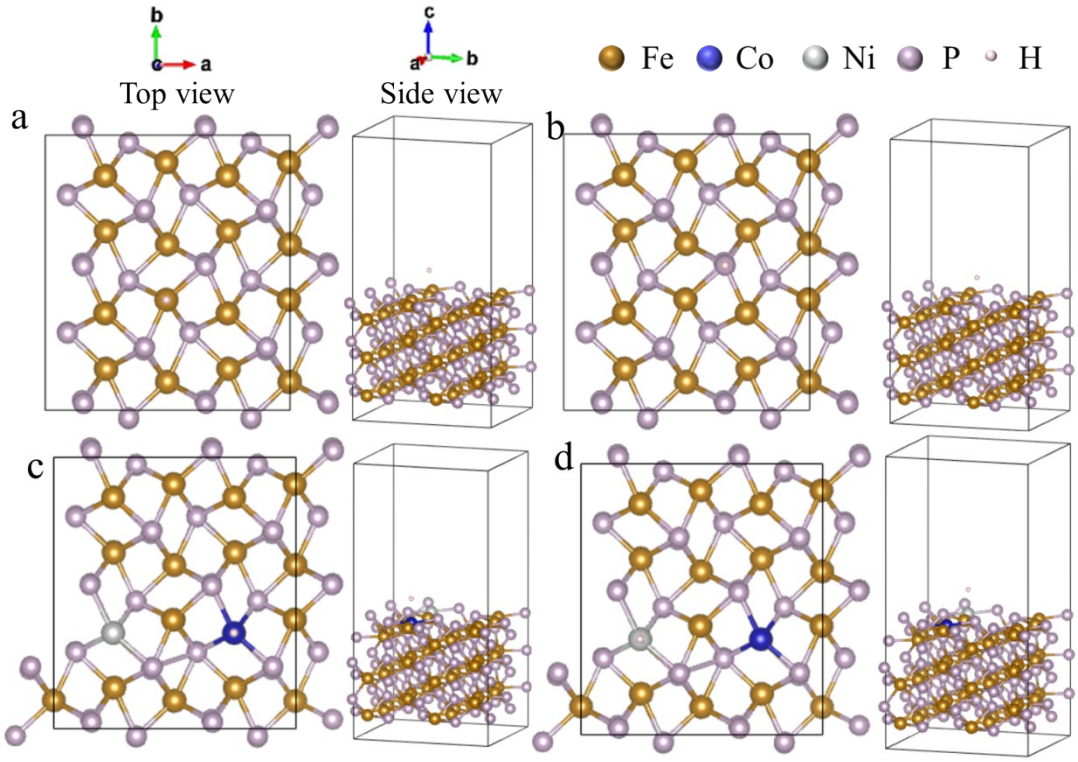

Fig. S8 Top and side view of (a, b) FeP (002) pristine structure and theoretical (c, d) Co/Ni doped FeP (002) model (gold: Fe, purple: Co, silver: Ni, gray: P, and white: H) before the optimization of hydrogen adsorption sites.

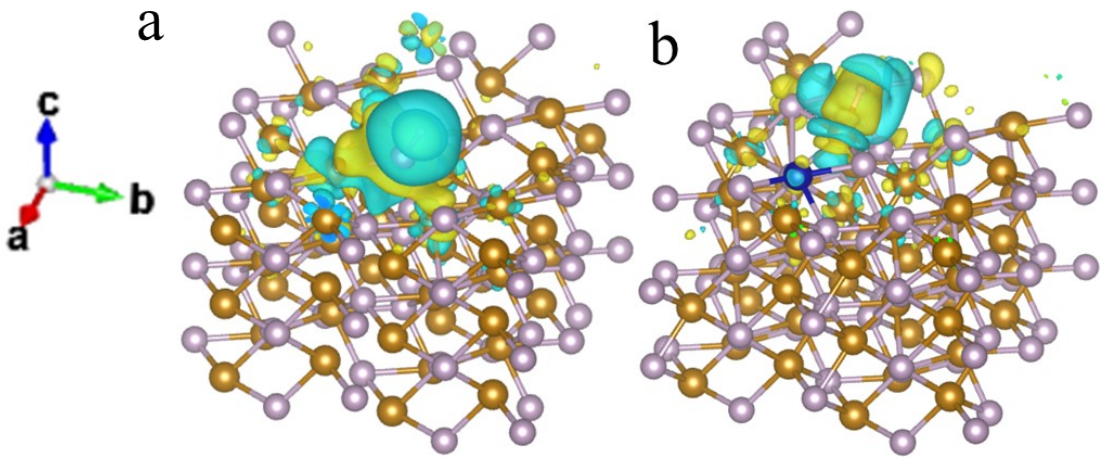

Fig. S9 The view sides for Bader charge analysis of FeP (002) (a) and Co/Ni doped FeP (002) (b) with optimal hydrogen adsorption site.

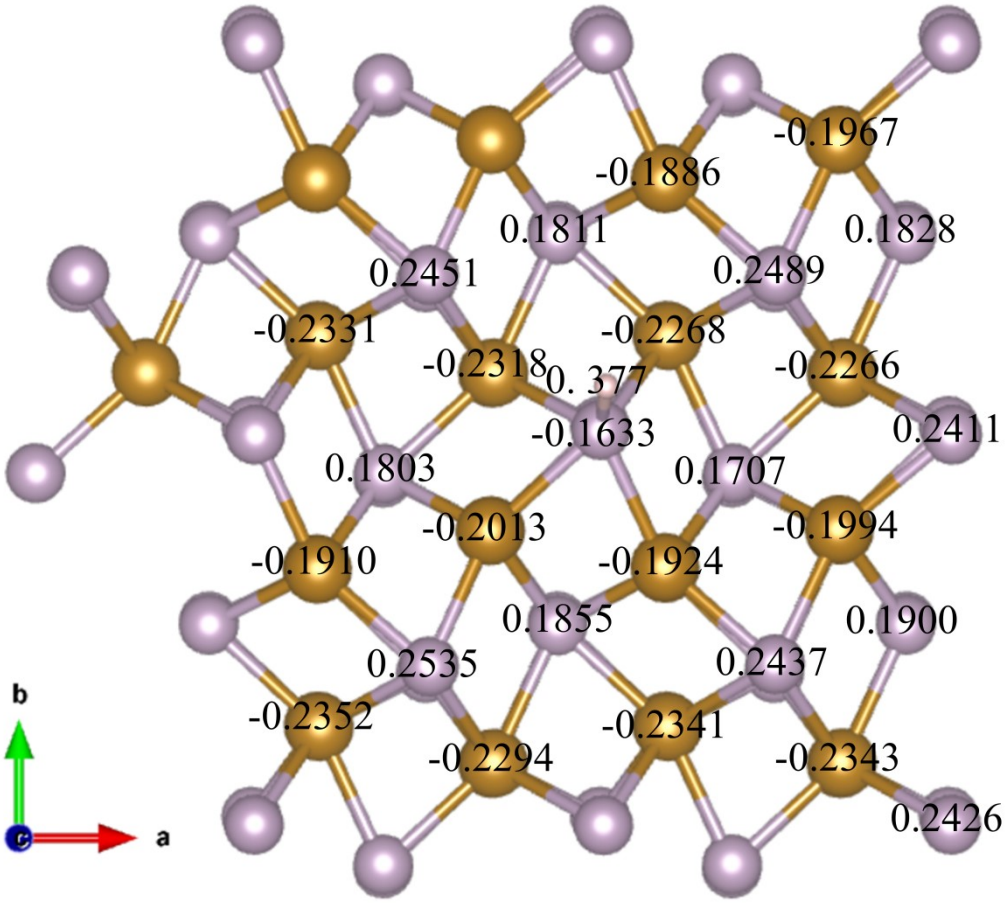

315

316

317 Fig. S10 The Bader charges of FeP (002).

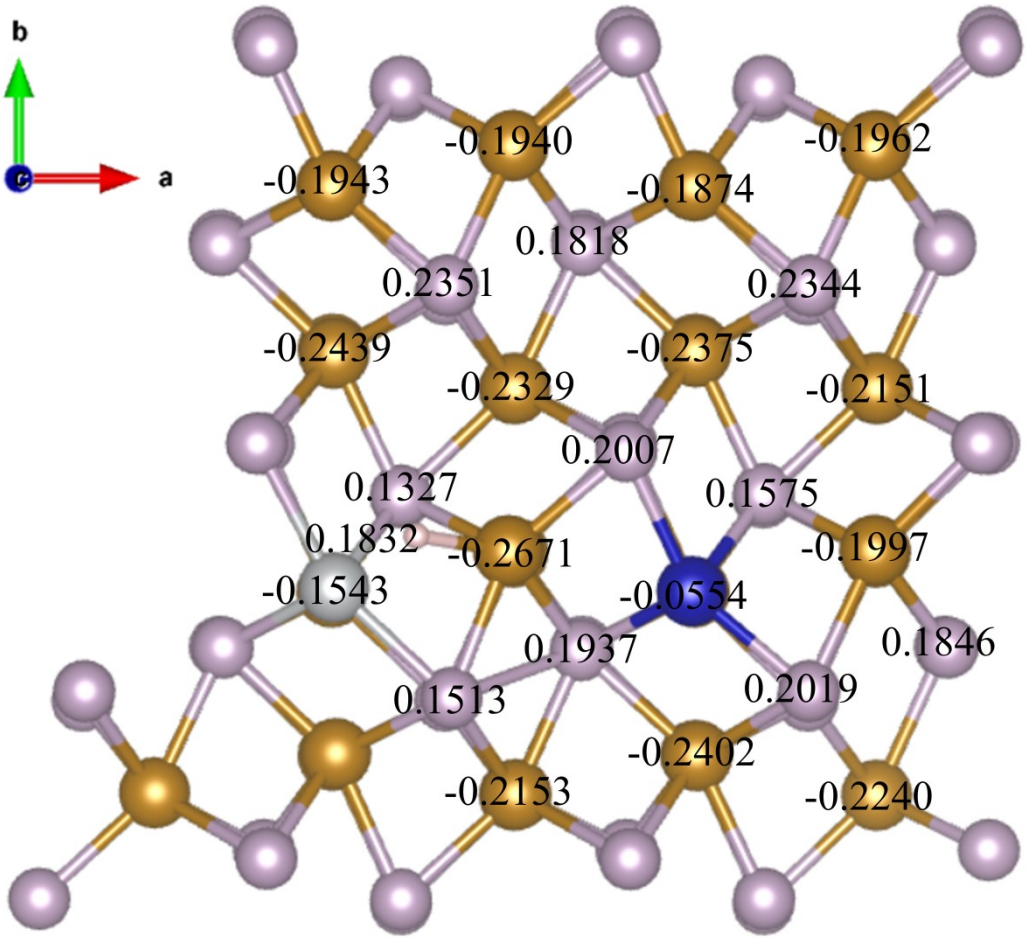

Fig. S11 The Bader charges of Co/Ni doped FeP (002).

Table S1. HER performance of catalysts with different ratios of dicyandiamide to FeCoNi-MOF-100 in 0.5 M H_2SO_4 and 1 M KOH.

Materials	0.5 M H_2SO_4		1 M KOH	
	Onset（mV）	η_{10}（mV）	Onset（mV）	η_{10}（mV）
0:1	124.3	210.8	227.4	307.1
0.5:1	114.2	215.4	269.4	413.2
1:1	42.7	110.3	142.3	239.4
1.5:1	135.7	320.0	251.3	404.0

Table S2. Electrocatalytic performance of catalysts with different calcination temperatures in 0.5 M H_2SO_4 and 1 M KOH.

Temperature (°C)	0.5 M H_2SO_4		1 M KOH	
	Onset（mV）	η_{10}（mV）	Onset（mV）	η_{10}（mV）
500	498.7	-	488.8	583.2
600	114.0	206.3	303.1	508.7
700	45.6	275.7	2965	503.4
800	42.7	110.3	145.2	239.4
900	114.2	231.3	275.1	469.0

Table S3. Electrocatalytic performance of catalysts with different calcination times in 0.5 M H_2SO_4 and 1 M KOH.

Time	0.5 M H_2SO_4		1 M KOH	
	Onset（mV）	η_{10}（mV）	Onset（mV）	η_{10}（mV）
1 h	70.8	147.1	177.8	267.8
2 h	24.2	86.7	132.4	233.5
3 h	85.7	169.8	221.1	320.1

Table S4. Electrocatalytic performance of catalysts with different ratios of mass ratio about sodium hypophosphite to the as-prepared FeCoNi-MOF-100@NCNTs in 0.5 M H_2SO_4 and 1 M KOH.

Materials	0.5 M H_2SO_4		1 M KOH	
	Onset（mV）	η_{10}（mV）	Onset（mV）	η_{10}（mV）
10:1	24.2	86.7	130.5	233.5
20:1	75.4	149.3	192.9	320.3
30:1	235.8	441.7	376.0	556.5

Table S5. Comparison of the HER performances of the related electrocatalysts reported recently.

Catalyst	Electrolyte	η_{10}/ mV	Tafel/ mV dec^{-1}	Stability	References
NCP@FeP_x	0.5 M H_2SO_4	96	50.16	a little attenuation after 2000 and 4000 cycles	1
MoO_2-FeP@C	0.5 M H_2SO_4	103	48	a negligible change after 5000 cycles very little attenuation after 24 h i-t test	2
FeP/MoS_2	0.5 M H_2SO_4	110	67.8	A negligible current decay at 30 mA cm^{-2} after 45 h i-t test	3
FeP/NCNSs	0.5 M H_2SO_4	114	64	A negligible degradation after 5000 cycles Insignificant fluctuations at 10 mA cm^{-2} after 20 h i-t test	4
$Co(OH)_2$/Ag/FeP	0.5 M H_2SO_4	118	79	No significant overpotential changes at 50 and 100 mA cm^{-2} after 50 h i-t test	5
NiPCM-101-450	0.5 M H_2SO_4	120	60.9	A slight degradation at 10 mA cm^{-2} after 4000s i-t test	6
Co-FeP NPs	0.5 M H_2SO_4	126	63.6	Significant current decay at 10 mA cm^{-2} after 1 h i-t test	7
La-MoP@NC	0.5 M H_2SO_4	129.3	57.9	Negligible current decay at 10 mA cm^{-2} after 1000 cycles A negligible current decay at 10 mA cm^{-2} after 12 h i-t test	8
Yb-MoP@NC		136.5	70.8	Negligible current decay at 10 mA cm^{-2} after 1000 cycles Significant current decay at 10 mA cm^{-2} after 12 h i-t test	
$Fe_{0.14}Co_{0.86}$-P/CC	0.5 M H_2SO_4	130	45.4	Negligible current decay after 2000 cycles	9

CoP/NCNHP	0.5 M H_2SO_4	140	53	A weak decay after 1000 cycles Significant current decay at 10 mA cm^{-2} after 24 h i-t test	10
Ni_2P/Ni@C	0.5 M H_2SO_4	149	61.2	Negligible current decay after 1000 cycles 89.0% retain at 10 mA cm^{-2} after 8 h i-t test	11
CoP-InNC@CNT	0.5 M H_2SO_4	153	62	93.6 % retain at 10 mA cm^{-2} after 20 h i-t test	12
NiFeP@C	0.5 M H_2SO_4	160	75.8	Significant current decay after 3000 cycles Significant current decay at 20 mA cm^{-2} after 30 h i-t test	13
Co/Ni-MOFs@P	0.5 M H_2SO_4	194	58.3	No significant overpotential changes at 10 mA cm^{-2} within 2000 min i-t test	14
FeCoNiP@NCNTs	0.5 M H_2SO_4	86.7	59.39	Without any obvious variation at 10 mA cm^{-2} after 20 h i-t test	This work

Table S6. Raw data of Bader charge analysis of FeP (002) with optimal hydrogen adsorption site.

Atom	x	y	z	Charge
1	6.75244	6.70697	10.90443	1.377
2	2.52588	1.73281	1.99991	7.73008
3	2.52588	1.73281	5.01059	7.778
4	2.55046	1.71325	8.05959	7.76482
5	2.5078	4.03417	3.50536	7.77817
6	2.5078	4.03417	6.51604	7.76427
7	2.52254	4.02251	9.27326	7.80896
8	5.0625	4.59506	3.50536	7.77798
9	5.0625	4.59506	6.51604	7.76454
10	5.04377	4.58508	9.28459	7.79872
11	5.08058	1.17192	1.99991	7.72986
12	5.08058	1.17192	5.01059	7.77662
13	5.10654	1.18432	8.04265	7.77062
14	7.63528	1.73281	1.99991	7.72973
15	7.63528	1.73281	5.01059	7.7782
16	7.65894	1.71313	8.07015	7.76591
17	7.6172	4.03417	3.50536	7.77801
18	7.6172	4.03417	6.51604	7.76254
19	7.61027	4.05503	9.25965	7.80763
20	10.1719	4.59506	3.50536	7.7781
21	10.1719	4.59506	6.51604	7.76567
22	10.16502	4.6115	9.30092	7.80057
23	10.18998	1.17192	1.99991	7.72988
24	10.18998	1.17192	5.01059	7.77665
25	10.21584	1.19145	8.05562	7.76572

26	2.52588	7.45731	1.99991	7.73022
27	2.52588	7.45731	5.01059	7.77749
28	2.55578	7.44133	8.05673	7.76687
29	2.5078	9.75867	3.50536	7.77848
30	2.5078	9.75867	6.51604	7.76357
31	2.50678	9.75156	9.29229	7.80414
32	5.0625	10.31956	3.50536	7.77825
33	5.0625	10.31956	6.51604	7.76364
34	5.05744	10.32092	9.29076	7.80438
35	5.08058	6.89642	1.99991	7.72986
36	5.08058	6.89642	5.01059	7.77705
37	5.11194	6.90777	8.06984	7.76818
38	7.63528	7.45731	1.99991	7.72992
39	7.63528	7.45731	5.01059	7.77601
40	7.66554	7.4428	8.01298	7.77324
41	7.6172	9.75867	3.50536	7.77853
42	7.6172	9.75867	6.51604	7.76239
43	7.61403	9.74725	9.27253	7.81144
44	10.1719	10.31956	3.50536	7.77811
45	10.1719	10.31956	6.51604	7.76284
46	10.16506	10.31526	9.28869	7.80329
47	10.18998	6.89642	1.99991	7.72977
48	10.18998	6.89642	5.01059	7.77703
49	0.00604	6.91112	8.0411	7.77342
50	3.48308	5.36672	1.99991	5.2632
51	3.48308	5.36672	5.01059	5.231
52	3.4852	5.42635	8.03553	5.1803
53	1.5505	0.40014	3.50536	5.21912
54	1.5505	0.40014	6.51604	5.22964
55	1.58972	0.2804	9.5534	5.24262
56	4.1052	2.50447	3.50536	5.21921

57	4.1052	2.50447	6.51604	5.22844
58	4.15664	2.60125	9.58935	5.25354
59	0.92838	3.26239	1.99991	5.2632
60	0.92838	3.26239	5.01059	5.2312
61	0.92642	3.21044	8.052	5.18996
62	8.59248	5.36672	1.99991	5.26387
63	8.59248	5.36672	5.01059	5.23133
64	8.60739	5.43419	8.03292	5.17069
65	6.6599	0.40014	3.50536	5.21914
66	6.6599	0.40014	6.51604	5.23083
67	6.71077	0.27283	9.5581	5.23933
68	9.2146	2.50447	3.50536	5.21952
69	9.2146	2.50447	6.51604	5.22846
70	9.22767	2.63447	9.55112	5.24374
71	6.03778	3.26239	1.99991	5.26329
72	6.03778	3.26239	5.01059	5.23133
73	6.03767	3.20053	8.04571	5.18549
74	3.48308	11.09122	1.99991	5.26321
75	3.48308	11.09122	5.01059	5.2309
76	3.48485	11.14735	8.04632	5.18275
77	1.5505	6.12464	3.50536	5.21907
78	1.5505	6.12464	6.51604	5.22918
79	1.60696	5.99631	9.56432	5.24106
80	4.1052	8.22897	3.50536	5.21906
81	4.1052	8.22897	6.51604	5.23241
82	4.15597	8.34018	9.56196	5.24511
83	0.92838	8.98689	1.99991	5.26303
84	0.92838	8.98689	5.01059	5.23023
85	0.936	8.92991	8.04519	5.18282
86	8.59248	11.09122	1.99991	5.26305
87	8.59248	11.09122	5.01059	5.2308

88	8.59846	11.14959	8.04456	5.18208
89	6.6599	6.12464	3.50536	5.21956
90	6.6599	6.12464	6.51604	5.23298
91	6.67135	6.06331	9.63017	4.83675
92	9.2146	8.22897	3.50536	5.21939
93	9.2146	8.22897	6.51604	5.22872
94	9.25144	8.33109	9.5372	5.24888
95	6.03778	8.98689	1.99991	5.26322
96	6.03778	8.98689	5.01059	5.2289
97	6.03769	8.92714	8.04294	5.18111

469

470 Table S7. Raw data of Bader charge analysis of Co/Ni doped FeP (002) with optimal hydrogen
471 adsorption site.

Atom	x	y	z	Charge
1	3.70008	4.8266	10.42497	1.1832
2	2.52588	1.73281	1.99991	7.72973
3	2.52588	1.73281	5.01059	7.77863
4	2.56481	1.7576	8.13125	7.75406
5	2.5078	4.03417	3.50536	7.77755
6	2.5078	4.03417	6.51604	7.77554
7	5.0625	4.59506	3.50536	7.77787
8	5.0625	4.59506	6.51604	7.76347
9	4.99687	4.61738	9.3924	7.73286
10	5.08058	1.17192	1.99991	7.7292
11	5.08058	1.17192	5.01059	7.77514
12	5.10692	1.1821	8.02517	7.78469
13	7.63528	1.73281	1.99991	7.73008
14	7.63528	1.73281	5.01059	7.77713
15	7.65663	1.72828	8.08883	7.75983
16	7.6172	4.03417	3.50536	7.77815
17	7.6172	4.03417	6.51604	7.75797
18	10.1719	4.59506	3.50536	7.77821
19	10.1719	4.59506	6.51604	7.75644
20	10.16027	4.62181	9.31725	7.80031
21	10.18998	1.17192	1.99991	7.72898
22	10.18998	1.17192	5.01059	7.77603
23	0.00968	1.20723	8.0634	7.76136
24	2.52588	7.45731	1.99991	7.72988
25	2.52588	7.45731	5.01059	7.7771

26	2.53901	7.39648	8.10442	7.75612
27	2.5078	9.75867	3.50536	7.77816
28	2.5078	9.75867	6.51604	7.76111
29	2.50381	9.75581	9.28452	7.80573
30	5.0625	10.31956	3.50536	7.77847
31	5.0625	10.31956	6.51604	7.76314
32	5.06115	10.3259	9.27999	7.80603
33	5.08058	6.89642	1.99991	7.72927
34	5.08058	6.89642	5.01059	7.77624
35	5.08956	6.90652	8.06441	7.76711
36	7.63528	7.45731	1.99991	7.72912
37	7.63528	7.45731	5.01059	7.77717
38	7.64244	7.41982	8.0866	7.76246
39	7.6172	9.75867	3.50536	7.7783
40	7.6172	9.75867	6.51604	7.76133
41	7.61884	9.75594	9.26756	7.81265
42	10.1719	10.31956	3.50536	7.7783
43	10.1719	10.31956	6.51604	7.76184
44	10.17057	10.32377	9.28285	7.80383
45	10.18998	6.89642	1.99991	7.7294
46	10.18998	6.89642	5.01059	7.77541
47	10.19842	6.90937	8.05623	7.78493
48	2.53842	4.09911	9.49721	9.84573
49	3.48308	5.36672	1.99991	5.26374
50	3.48308	5.36672	5.01059	5.22961
51	3.48177	5.39265	8.0181	5.13272
52	1.5505	0.40014	3.50536	5.21949
53	1.5505	0.40014	6.51604	5.24014
54	1.58707	0.27866	9.57502	5.25021
55	4.1052	2.50447	3.50536	5.21939
56	4.1052	2.50447	6.51604	5.22799

57	4.19502	2.54196	9.54912	5.15132
58	0.92838	3.26239	1.99991	5.26356
59	0.92838	3.26239	5.01059	5.23459
60	0.97071	3.25104	8.08953	5.1846
61	8.59248	5.36672	1.99991	5.26286
62	8.59248	5.36672	5.01059	5.22952
63	8.59634	5.41573	8.04294	5.1575
64	6.6599	0.40014	3.50536	5.21959
65	6.6599	0.40014	6.51604	5.23411
66	6.71097	0.27138	9.56403	5.23416
67	9.2146	2.50447	3.50536	5.21886
68	9.2146	2.50447	6.51604	5.23489
69	9.23781	2.6389	9.5386	5.2019
70	6.03778	3.26239	1.99991	5.26237
71	6.03778	3.26239	5.01059	5.2314
72	6.01479	3.21466	8.0636	5.19372
73	3.48308	11.09122	1.99991	5.26324
74	3.48308	11.09122	5.01059	5.22865
75	3.48351	11.15355	8.04866	5.1885
76	1.5505	6.12464	3.50536	5.21863
77	1.5505	6.12464	6.51604	5.22279
78	1.45386	6.12833	9.6506	5.19433
79	4.1052	8.22897	3.50536	5.22047
80	4.1052	8.22897	6.51604	5.23174
81	4.14234	8.35494	9.56581	5.23514
82	0.92838	8.98689	1.99991	5.26242
83	0.92838	8.98689	5.01059	5.232
84	0.93527	8.91925	8.05195	5.18281
85	8.59248	11.09122	1.99991	5.26244
86	8.59248	11.09122	5.01059	5.23043
87	8.60395	11.16223	8.04423	5.18634

88	6.6599	6.12464	3.50536	5.21912
89	6.6599	6.12464	6.51604	5.22964
90	6.6597	6.01756	9.58203	5.20074
91	9.2146	8.22897	3.50536	5.21957
92	9.2146	8.22897	6.51604	5.23259
93	9.25345	8.35444	9.56396	5.23436
94	6.03778	8.98689	1.99991	5.26265
95	6.03778	8.98689	5.01059	5.23169
96	6.03851	8.9205	8.04851	5.18178
97	7.58202	4.0453	9.27537	8.94465

References

[1] M. Li, X. Liu, X. Hu, Fabrication of core-sheath NiCoP@FeP_x nanoarrays for efficient electrocatalytic hydrogen evolution, *ACS Sustain. Chem. Eng*., 2018, **6**, 8847-8855.

[2] G. Yang, Y. Jiao, H. Yan, Interfacial engineering of MoO_2-FeP heterojunction for highly efficient hydrogen evolution coupled with biomass electrooxidation, *Adv. Mater*., 2020, **32**, 2000455.

[3] M. H. Suliman, A. Adam, L. Li, FeP/MoS_2 enriched with dense catalytic sites and high electrical conductivity for the hydrogen evolution reaction, *ACS Sustain. Chem. Eng*., 2019, **7**, 17671-17681.

[4] Y. Yu, Z. Peng, M. Asif, FeP nanocrystals embedded in N-doped carbon nanosheets for efficient electrocatalytic hydrogen generation over a broad pH range, *ACS Sustain. Chem. Eng*., 2018, **6**, 11587-11594.

[5] X. Ding, Y. Xia, Q. Li, Interface engineering of $Co(OH)_2$/Ag/FeP hierarchical superstructure as efficient and robust electrocatalyst for overall water splitting, *ACS Appl. Mater. Inter*., 2019, **11**, 7936-7945.

[6] O. Mabayoje, S. G. Dunning, K. Kawashima, Hydrogen evolution by Ni_2P catalysts derived from phosphine MOFs, *ACS Appl. Energ. Mater*., 2019, **3**, 176-183.

[7] G. Cho, Y. Park, H. Kang, Transition metal-doped FeP nanoparticles for hydrogen evolution reaction catalysis, *Appl. Surf. Sci*., 2020, **510**, 145427.

[8] P. Wei, X. Li, Z. He, Electron density modulation of MoP by rare earth metal as highly efficient electrocatalysts for pH-universal hydrogen evolution reaction, *Appl. Catal. B-Environ*., 2021, **299**, 120657.

[9] H. Yu, L. Qi, Y. Hu, Nanowire-structured FeP-CoP arrays as highly active and stable bifunctional electrocatalyst synergistically promoting high-current overall water splitting, *J. Colloid. Interf. Sci*., 2021, **600**, 811-819.

[10] Y. Pan, K. Sun, S. Liu, Core-shell ZIF-8@ZIF-67-derived CoP nanoparticle-embedded N-doped carbon nanotube hollow polyhedron for efficient overall water

splitting, *J. Am. Chem. Soc*., 2018, **410**, 2610-2618.

[11] X. Liu, W. Li, X. Zhao,Two birds with one stone: metal-organic framework derived micro-/nanostructured Ni_2P/Ni hybrids embedded in porous carbon for electrocatalysis andenergy storage, *Adv. Funct. Mater*., 2019, **29**, 1901510.

[12] L. Chai, Z. Hu, X. Wang, Stringing bimetallic metal-organic framework-derived cobalt phosphide composite for high-efficiency overall water splitting, *Adv. Sci*., 2020, **7**, 1903195.

[13] Q. Kang, M. Li, J. Shi, A universal strategy for carbon-supported transition metal phosphides as high-performance bifunctional electrocatalysts towards efficient overall water splitting, *ACS Appl. Mater. Inter*., 2020, **12**, 19447-19456.

[14] P. Luo, Z. Pang, Z. Qin, Strategies for improving Co/Ni-based bimetal-organic framework to water splitting, *Int. J. Hydrogen Energ*., 2020, **45**, 28240-28251.